Adsorption of human serum albumin: Dependence on molecular architecture of the oppositely charged surface

Svetlana A. Sukhishvili and Steve Granick
Department of Materials Science and Engineering, University of Illinois at Urbana-Champaign, Urbana, Illinois 61801

(Received 8 December 1998; accepted 26 February 1999)

We contrast the adsorption of human serum albumin (HSA) onto two solid substrates previously primed with the same polyelectrolyte of net opposite charge to form one of two alternative structures: randomly adsorbed polymer and the ''brush'' configuration. These structures were formed either by the adsorption of quaternized poly-4-vinylpyridine (QPVP) or by end-grafting QPVP chains of the same chemical makeup and the same molecular weight to surfaces onto which QPVP segments did not adsorb. The adsorption of HSA was quantified by using Fourier transform infrared spectroscopy in attenuated total reflection (FTIR-ATR). The two substrates showed striking differences with regard to HSA adsorption. First, the brush substrate induced lesser perturbations in the secondary structure of the adsorbed HSA, reflecting easier conformational adjustment for longer free segments of polyelectrolyte upon binding with the protein. Second, the penetration of HSA into the brush substrate was kinetically retarded relative to the randomly adsorbed polymer, probably due to both pore size restriction and electrostatic sticking between charged groups of HSA and QPVP molecules. Third, release of HSA from the adsorbed layer, as the ionic strength was increased from a low level up to the high level of 1 M NaCl, was largely inhibited for the brush substrate, but occurred easily and rapidly for the substrate with statistically adsorbed QPVP chains. Finally, even after addition of a strong polymeric adsorption competitor (sodium polystyrene sulfonate), HSA remained trapped within a brush substrate though it desorbed slowly from the preadsorbed QPVP layer. This method to produce irreversible trapping of the protein within a brush substrate without major conformational change may find application in biosensor design. © *1999 American Institute of Physics.* [S0021-9606(99)50120-7]

INTRODUCTION

Binding of proteins to a surface lies at the heart of a multitude of events in the fields of biology and technology. Protein membrane, protein-chromatographic surface, and protein-latex particle binding are just a few examples of these common interactions. The areas of practical implication range from large-scale industrial to analytical chromatographic separations of proteins,[1–4] latex agglutination tests,[5] traditional enzyme biosensors,[6] and recently proposed multiprotein biosensors fabricated by layer-by-layer adsorption of polyelectrolytes and proteins or enzymes.[7,8]

The binding of proteins to a surface or gel, or to another macromolecule, comprises a complex sequence of events that includes changes of the local charge and local dielectric environment. Most of the academic literature on these matters, however, concerns the ultimate global effect of these perturbations−conformational changes of proteins, with the emphasis on the adsorption to initially-bare solid hard substrates[9–18] and the activity of bound enzymes,[19–21] in spite of the fact that in many recent applications, biological molecules interact with surfaces that have previously been modified by polymers, especially polyelectrolytes. This situation is especially common in the fields of biosensors and ion-exchange chromatography.[22,23] Some studies have shown that surface modification of this kind yields lessened adsorption-induced conformational distortion of protein structure—thus promising a potential advantage over hard, solid surfaces.[18]

In seeking to understand observations of this kind, there are many open questions. How does molecular conformation of the adsorbate adapt to the local structure of the surface? How in turn does this influence the adsorbent's conformation? In these processes, what is the role of the molecular architecture of the substrate? Is it possible, by changing the molecular architecture of the substrate, to directly modify such properties as conformational changes and strength of the uptake of the biomolecules by the substrate?

In this article, we study the binding of a model protein (human serum albumin, HSA) with responsive substrates of two types: (1) silicon (Si) crystals coated by a statistically adsorbed layer of a synthetic polymer, quaternized poly-4-vinylpyridine, QPVP, of opposite Coulombic charge; and (2) hydrophobized Si crystals coated with this same charged polymer but arranged in the end-on (grafted) configuration to comprise a polyelectrolyte brush rather than a statistically-adsorbed structure (the procedure for synthesis of the polyelectrolyte grafts is described elsewhere). Among these two cases, case (1), the statistically adsorbed structure, is reminiscent of the polyelectrolyte matrices commonly used to bind macromolecules in biotechnology applications.[22] Case (2), the polyelectrolyte brush, is more pure conceptually and incidentally is also reminiscent of ''tentacular'' ion-

exchange beads currently sold by Merck.[23] We are interested to understand the binding and conformation of HSA with these two surfaces, with emphasis on the influence of the substrate architecture on the ease of HSA desorption in the presence of high concentrations of inorganic salts or in the presence of polyelectrolyte adsorption competitors.

The HSA molecule is a multidomain protein with well-known amino-acid composition and structure.[24] The reported isoelectric point of HSA is 5.2.[25] The HSA globule has been traditionally considered as a prolate ellipsoid with the maximum length and width of about 14 to 4 nm,[9,26] but recent NMR study of the protein also suggests a triangular shape with sides of about 8 nm and average thickness of 3 nm.[24]

EXPERIMENT

Materials

Human serum albumin (HSA) was selected because this well-studied model protein is readily available. It was purchased from Aldrich–Sigma and was used without further purification.

Many experiments were performed in D_2O rather than H_2O for reasons discussed below; we refer then to *p*D rather than *p*H. To control *p*D and ionic strength, the inorganic salts Na_2HPO_4, $NaH_2PO_4^*H_2O$ and NaCl (General Storage, pure grade) were used as received.

The H_2O used for glassware cleaning was double distilled and further purified by passage through a deionizing Milli-Q System (Millipore). To reduce overlap of the infrared (IR) spectra of Amide I band with the strong water band, we used D_2O with 99.9% isotope content. This solvent was purchased from Cambridge Isotope Laboratories and was used as received. Control experiments showed no difference when using purified H_2O, thus confirming purity of the as-received D_2O.

The polymers used for end grafting and statistical adsorption onto the silicon surfaces are described below.

For displacement with polystyrene sulfonate (PSS), the completely sulfonated sodium salt of PSS was purchased from Polymer Laboratories and used as received. The weight-average molecular weight was $M_w = 35\,000$ g mol^{-1} and the ratio of weight-average to number-average molecular weight was stated to be $M_w/M_n = 1.1$.

FTIR-ATF spectroscopy

Infrared spectra were collected using a Biorad FTS-60 Fourier transform infrared spectrometer (FTIR) using a Biorad FTS-60A spectrometer equipped with a mercury-cadmium-telluride detector and a home-built adsorption cell.[27] Attenuated total reflection (ATR) optics and the thermostatted cell were described previously.[27] By switching a wire-grid polarizer (Graesby/Specac), the spectra in both *p* and *s* polarization were obtained.

The temperature was 25.0°C. The underlying surface was a rectangular trapezoidal Si crystal of dimension 50 mm×20 mm×2 mm with angle 45° to the incident beam and with 45° angle to the incident infrared beam.

Each absorbance spectra was ratioed to a corresponding background, measured in the same polarization of the incident beam taken with D_2O buffer solutions containing the same concentration of inorganic salts as in the sample solution. Interferograms for both *p* and *s* polarization were collected with 4 cm^{-1} resolution. For experiments concerning time dependence of the amount adsorbed, the number of scans during the first 6 min was 24, then 128 for the subsequent 10 min and 256 or 512 for longer times. For static experiments, the number of scans was 512. Occasionally, measurements were performed using nonpolarized light. In the setup of our experiment, the intensities of the incident beam polarized in *p* and *s* directions were equal, and the absorbances measured with nonpolarized light (A) and those obtained for *p* and *s* polarization (A_p and A_s) satisfied the following simple relationship expected from geometric optical considerations:

$$A = (A_p + A_s)/2. \tag{1}$$

Ellipsometric measurements

Measurements concerning the dry film of grafted PVP polyelectrolyte were performed using a Gaertner Model L116C ellipsometer with He/Ne laser at 70° angle of incidence. Before depositing the polymer grafts, real and imaginary parts of the refractive index of the substrate bearing the layer of self-assembled molecules, n_s and K_s, were measured. Thickness of the grafted layer was then calculated using Gaertner software for one layer assuming the refractive index of 1.55 for the neutral grafted PVP layer.

Preparation of the Si surfaces for the adsorption of HSA

In this work, we used two different strategies to modify the surface of a Si crystal with polycationic polymer, QPVP. The first was to attach this polyelectrolyte in the end-grafted conformation, as a polyelectrolyte brush, onto an otherwise hydrophobically modified Si surface onto which the polymer did not adsorb except where grafted.[28] The second was to allow quaternized PVP polymer to adsorb spontaneously onto the silicon oxide surface, forming statistically adsorbed layers. Since in this latter case each segment had a finite statistical likelihood of adsorption, this method produced more ''flattened'' polyelectrolyte layers.

Preparation of substrate

Deposition and characterization of polyelectrolyte brushes

Polyelectrolyte brushes were deposited, using the procedure described in our earlier paper,[28] onto a flat, 45° trapezoidal 50×20×2 mm silicon ATR crystal (Harrick Corp.) that had previously been coated with a monolayer of olefin-terminated condensed triethoxysilane. In brief, styrenyl-terminated poly-4-vinylpyridine (s-PVP) with degree of polymerization ≈60 ($M_w/M_n = 1.17$) (Polymer Source, Canada) was grafted to a monolayer of olefin-terminated self-assembled monolayer using UV (ultraviolet) light (step 1). The grafting density was easily controlled at this

step by the choice of different concentrations of the s-PVP solution, as described previously. [28] After grafting, the resulting uncharged chains were alkylated with excess methyl iodide (15% by volume in dimethylformamide) for 1 h at room temperature (step 2) to achieve the maximum attainable conversion of pyridine into pyridinium rings (98%) and finally, the I^- counterion was exchanged for Br^- (step 3). The grafting densities reported below, calculated from either FTIR-ATR or ellipsometric measurements of dry films, gave consistent results. Note that in this work, the maximum amount of the grafted PVP was ≈35% larger than we previously reported,[28] possibly because the heavier quartz slide used in this study resulted in a smaller gap between the quartz and crystal surfaces and therefore a higher grafting efficiency from UV irradiation.

To calibrate the adsorbed amount, the following procedures were employed, as summarized in more detail elsewhere.[29] The basic measurement was the sum of integrated FTIR-ATR absorbances of characteristic infrared bands for *p*- and *s*-polarized incident beams. To convert this sum, $A_p + A_s$, to the amount adsorbed, we used the calibration constant 0.028 abs units m^2 mg^{-1} for the completely alkylated PVP. We also used the additional calibration coefficient of 0.55 to account for the fact that the portion of Si crystal covered with QPVP brush was larger than that exposed to the QPVP solution in the original calibration experiment.

Deposition of the polyelectrolyte by adsorption

The polyelectrolyte used for statistical adsorption was essentially the same chemically as the polyelectrolyte brush. It was obtained from the parent poly-4-vinylpyridine (PVP) ($M_w = 34\,000$, $M_w/M_n = 1.23$), which was purchased from Polymer Source, Canada. The procedure to quaternize PVP with an excess of ethyl bromide was described by us elsewhere.[29] The proportion of alkylated units in the yielded polymer was 98%. The resulting polymer is referred to, in this paper, as QPVP.

Adsorption of QPVP onto the surface of freshly cleaned oxidized Si is described elsewhere.[30] The amount of QPVP adsorbed was controlled by proper choice of pD for deposition. In a typical route, 0.2 mg mL^{-1} solution of QPVP in 0.003 M borate or phosphate buffer was allowed to adsorb to the surface of the Si crystal for 30 min, and after that polymer solution was displaced to a pure buffer solution. QPVP did not desorb after initial adsorption: neither into the pure buffer (neither at the same nor at different pD), nor after the subsequent adsorption of HSA.

Calibration of the amount adsorbed of HSA

Calibrations of the amount adsorbed were performed based on measuring the infrared absorbance of known quantities of oscillators in solution. This basically followed the method described previously[30,31] and was based on integrating the product of the amplitude of the evanescent wave and the concentration of the absorbing species as a function of distance from the crystal surface, yielding the integrated absorbance of the relevant IR peak.[32,33] For the 45° angle of incidence at silicon that we used, the penetration depth of the evanescent wave was 0.47 μm at 1643 cm^{-1} wave number.

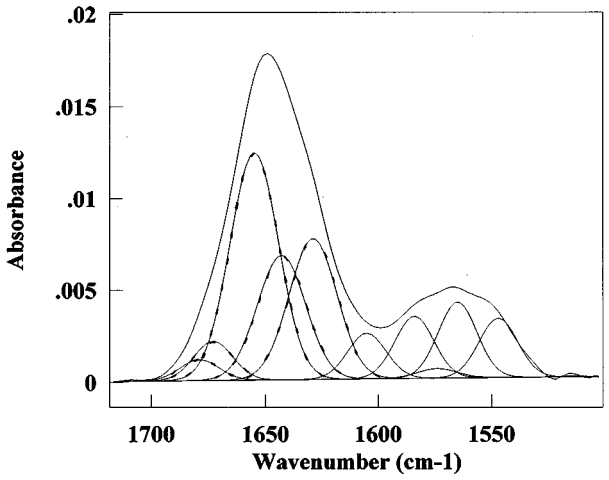

FIG. 1. Infrared absorption spectrum of human serum albumin, HSA, at concentration 10 mg mL^{-1}solution in buffered D_2O solution. The absorption modes shown in dotted lines were used to infer the protein conformations and additional adsorption modes (see text and Table I). Composition of the buffer was 3 mM $Na_2B_4O_7^*10H_2O$, pD=9.2.

Calibration of the amount adsorbed of HSA from integrated infrared peaks was performed based on the total intensity of the amide I peak. The calibration constant was determined from an experiment in which absorbing species were brought into contact with a nonadsorbing surface. In this paper, we used two different but consistent methods of calibration. In method I, a bare surface of oxidized Si crystal was used a substrate, since at pD=9.2 (commonly employed in subsequent experiments), the amount of HSA adsorbed on the Si surface was only 0.035 mg m^{-2} for the highest solution concentration of HSA, 14 mg mL^{-1}, so that this surface could be considered as essentially nonadsorbing. For completeness, the small portion of intensity originating from adsorbed protein was subtracted from the total intensity. A different method to produce a nonadsorbing surface (method II) was based on the observation that the quantity of HSA adsorbed on either preadsorbed QPVP or PVP brush saturated as the concentration of HSA in solution was raised (see below). Subsequent increase of inferred absorbance with increasing solution concentration of HSA could be attributed to the oscillators in the solution only.

For the 50 mm×20 mm×2 mm Si crystal used in these experiments, methods I and II gave consistent values of the calibration constants, 0.467 and 0.484 abs units m^2 mg^{-1}, respectively. We used their average, 0.475 abs units m^2 mg^{-1}, to infer the mass adsorbed.

We also found that absorbance of this amide I band did not change when salt concentration was varied from 0.003 to 1.5 M NaCl, suggesting that the molecular absorptivity of HSA did not depend on the salt concentration.

RESULTS AND DISCUSSION

Representative spectra

Figure 1 shows the spectra of HSA taken in D_2O containing 0.003 M borax to produce pD=9.2. Absorbance is plotted against wave number in the infrared spectrum. In

TABLE I. Secondary structure of HSA in solution, 10 mg mL^{-1}, pD 9.2 (0.003 M borate buffer). Note that the percentage of turns, α helix, β sheet, and unordered structure was calculated as the ratio of the corresponding peak areas to the total area of all five amide I peaks.

Peak	Center (cm^{-1})	Structural assignment	Fixed bandwidth (cm^{-1})	%[a] (Gaussian to Lorenzian ratio is shown)	% (Gaussian fit)
1	1679	turns	15	0.8 (9999:1)	1.3
2	1673	turns	15	0.3 (9999:1)	0
3	1655	α helix	30	64 (7:3)	56
4	1643	unordered	20	14.5 (9999:1)	11.9
5	1629	β sheet	30	20.5 (9999:1)	30.8

these experiments, solutions of HSA were exposed to the surface modified by QPVP brush, which was already saturated with protein at pD 9.2; the measured absorbance originated only from molecules free in solution since HSA did not adsorb onto the surface.

The spectrum shows a characteristic amide I region (1610–1690 cm^{-1}). This region is widely used for the conformational analysis of globular proteins.[34–37] Comparing the literature data on the amide I frequencies of hydrogenated HSA with our results, one can conclude that hydrogen-to-deuterium exchange did not shift the position of the amide I peak by more than by 2 cm^{-1}. This is consistent with the small shifts (from 3 to 10 cm^{-1}) to lower wavenumber that have been reported for various polypeptides and proteins.[38,39] Isotope exchange had a much stronger effect on the position of the amide II band, which is caused by NH vibration, and usually is observed around 1550 cm^{-1}in water. The frequency of this band was shifted to 1450 cm^{-1} after isotope exchange of hydrogen to deuterium and was not in the frequency range measurable with a Si ATR crystal (opaque at wavenumbers below 1500 cm^{-1}). The absorbance at 1550 cm^{-1} (the location of the amide II band in H_2O) was very weak, suggesting almost complete exchange of NH to ND functions during the 1 h elapsed between measurement and preparation of the D_2O solutions. The overlapping peaks at 1584, 1574, and 1565 cm^{-1} corresponded to the stretching vibrations of the carboxylate groups (ν_{aCOO})of Asp and Glu residues. This broad band was relatively weak for HSA since this protein contains only a small proportion of Asp and Glu.

The peaks of HSA were integrated by curve-fitting using Spectracalc software. After spectra deconvolution, peak assignments were made using abundant data on the subject reported elsewhere.[35–38] The wide amide I band of HSA was decomposed into five components, associated with the various structures in which carbonyl groups are involved: turns (1679 and 1673 cm^{-1}), α-helix (1655 cm^{-1}), unordered structure (1643 cm^{-1}) and β sheet (1629 cm^{-1}). At lower frequencies, four more components were introduced, associated with aromatic side chains (1595 cm^{-1}) and carboxylate function (1584, 1574, and 1565 cm^{-1}) vibrations; we did not use them in our analysis. For curve fitting, we used a parameter file in which band centers and widths, as well as Gaussian-to-Lorentzian ratio, were fixed for each band. These levels for five amide I peaks are shown in Table I. The same parameters were applied to all the spectra. Note the consistency of our results: application of a similar parameter file, but with purely Gaussian shapes of the bands, introduced slight quantitative differences (see table I) but did not change the main result.

Conformational analysis of HSA on different substrates

In this section, we are concerned with the question: How do conformational changes of the protein upon adsorption depend on the molecular architecture of the substrate? The notion that adsorption onto a solid surface produces conformational distortions relative to the native (solution) conformation has a long history. In particular, the entropy gain resulting from surface-induced conformational changes has been found to contribute to the driving force for adsorption, especially in the case of the proteins with low structural stability as HSA.[40,41]

Table II compares IR measurements of the conformational distortions of HSA induced by the two types of the substrates, statistically adsorbed QPVP polyelectrolyte and the QPVP polyelectrolyte brush. On both substrates, secondary structure of the protein was distorted: the portion of turns and unordered motifs increased at the expense of α-helical structure. However, one notices a distinct difference in the degree of the distortion: for the brush substrate, the conformational changes were less. This conclusion held for comparisons in which the amount of QPVP was similar: for the QPVP brush, $\Gamma_{QPVP}=1.8$ mg m^{-2} and for the statistically adsorbed QPVP, $\Gamma_{QPVP}=1.7$ mg m^{-2}, as shown in Table II. Similar conclusions (not shown) held for the brush substrate with $\Gamma_{QPVP}=2.3$ mg m^{-2}.

Because the maximum amount of adsorbed HSA also differed according to the substrate (see Fig. 3), we carefully examined the influence of this variable, but found that the

TABLE II. ATR-FTIR analysis of the change in secondary structure of HSA upon adsorption onto the two substrates. In parenthesis, the results of Gaussian fit are shown.

	Solution	HSA in the QPVP brush; $\Gamma_{QPVP}=1.8$ mg/m^2	HSA on the QPVP adsorbed; $\Gamma_{QPVP}=1.7$ mg/m^2
α helix, %	64 (56)	55.3 (53.1)	52.5 (51.5)
turns, %	1 (1)	2.7 (3)	3.8 (5)
unordered, %	14.5 (10.1)	18.5 (10.9)	20.7 (10.6)
β sheet, %	20.5 (32.9)	23.8 (33)	23.1 (32.9)

conformational distortions did not change within experimental uncertainty when the HSA surface coverage was varied within a wide range, from 1.95 to 2.8 mg m^{-2} for the statistically adsorbed substrate and from 2.2 to 6 mg m^{-2} for the brush substrate. *In toto*, the results suggest that QPVP chains provided a less disturbing environment for the HSA when they were grafted to the surface than when they were adsorbed.

This probably reflected the larger extension of the polyelectrolyte chains from the surface in the former case, and their associated higher flexibility/conformational freedom at the time of interaction with the protein globules. The QPVP chains could then more readily adjust conformation during complex formation without requirement that the protein globule do so. The limiting case of this kind of situation would be complexation with polyelectrolyte chains free in solution. Indeed, one notes that hardly any conformational changes of protein structure were observed upon the complexation of the similar protein, bovine serum albumin (BSA), with polyelectrolyte in solution.[42]

It might seem surprising at first glance that the brush substrate had the milder effect on HSA, given that the hydrophobicity of the self-assembled monolayer beneath the grafted brush might itself be expected to induce major conformational distortion.[43] Two points should be noted. First, HSA had low affinity for this self-assembled layer: only 0.35 mg m^{-2} would adsorb (at pD=9.2, from [HSA]=1 mg mL^{-1} in solution), a quantity 6 to 17 times less than on the QPVP-modified substrates. Second, one might have naively expected the affinity of the protein for this ''organic carpet'' to rise as a result of hydrophobization of the brush layer upon absorption of HSA molecules. But this conceivable influence was evidently inhibited by the structural hindrance of the grafted chains.

Adsorbed amount compared for the two substrates and demonstration of electrostatically driven adsorption

At pD=9.2, the negatively charged HSA globules encountered electrostatic affinity to the positively charged surface. Figure 2 shows the adsorption isotherms under conditions where the quantity of surface-bound QPVP was the same. One notes that for both substrates, physisorbed polymer and end-grafted chains, the plateau in the amount adsorbed set in above the concentration of about 0.1 mg mL^{-1}. This agrees with data reported for other substrates.[44] At the same time, the amount of the adsorbed HSA on the brush substrate exceeded that on the substrate with physisorbed polymer.

Now we focus on correlations between the amount of HSA adsorbed and the amount of the QPVP bound to the substrate surface. Figure 3 shows this correlation for both types of substrates. Adsorbed amount is plotted against mass of QPVP on the surface. The latter was determined both by ellipsometric thickness of dried neutral PVP and ATR-FTIR spectroscopy; details of these measurements are described in Experimental section. Two points are evident in Fig. 3. First, the more QPVP was bound to the substrate surface, the more HSA adsorbed; the correlation between these quantities appears to be linear. Second, one notices that in a comparison concerning the same amount of QPVP adsorbed on the two types of substrates, more HSA adsorbed onto the brush (≈30–35% more).

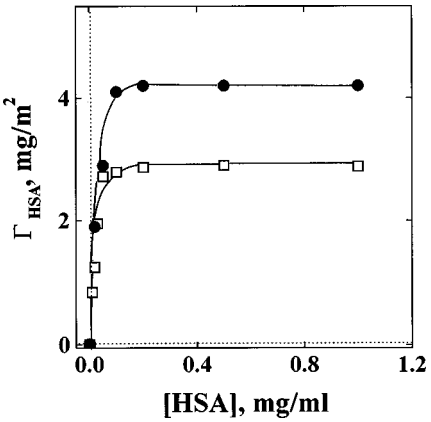

FIG. 2. Adsorption isotherm of HSA onto two substrates with matched amount of QPVP on the surface. QPVP chains were either statistically adsorbed on the surface (open squares, QPVP adsorbed amount 1.7 mg m^{-2}), or chemically grafted (filled circles, QPVP grafted amount 1.8 mg m^{-2}). The buffer solution was the same as in Fig. 1, pD=9.2.

Enhanced adsorption onto the brush probably reflects the fact that when QPVP adsorbed, it did so with a significant fraction of segments on the solid surface itself, leaving fewer segments available for subsequent binding with HSA.

Confirmation of the electrostatic mechanism of adsorption also came from studies of mass adsorbed as a function of the ionic strength in bulk solution. In Fig. 4, relative HSA adsorption (mass adsorbed normalized by initial mass adsorbed) is plotted against elapsed time as the adsorbed layer was exposed to buffer solutions with different concentrations of NaCl. The different response according to the substrate (a QPVP brush, 1.8 mg m^{-2}, and a statistically adsorbed QPVP, 1.7 mg m^{-2}) is striking. From the latter, HSA was easily and rapidly desorbed after the NaCl concentration was raised, without subsequent changes in the amount adsorbed after an equilibration time of 5 min. In contrast, desorption from the QPVP brush was largely inhibited: only 5% of the

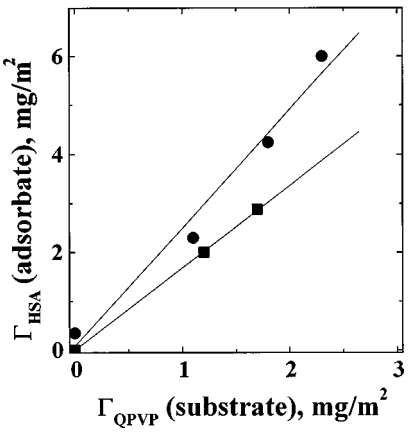

FIG. 3. Maximum mass adsorbed of HSA is plotted against quantity of QPVP grafted to the surface (filled circles) or adsorbed to the surface (filled squares). The buffer solution was the same as in Fig. 1, pD=9.2.

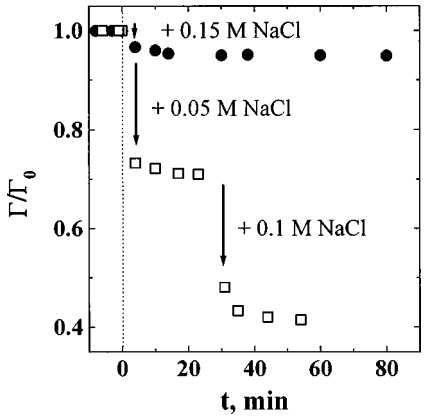

FIG. 4. Normalized mass adsorbed of HSA (relative to the initial amount adsorbed before additional salts were added, Γ_0) is plotted against elapsed time after exposing two different substrates to buffer solutions with higher ionic strengths as written in the figure. Adsorption onto the brush substrate is denoted by filled circles. Adsorption onto the substrate with preadsorbed QPVP is denoted by open squares. In both cases, HSA was first allowed to adsorb onto the substrate surfaces from 1 mg mL^{-1} solution at pD=9.2 for 30 min at low-salt conditions (pure buffer, 3 mM $Na_2B_4O_7^*10H_2O$, pD 9.2) until the saturated amount Γ_0 of the protein was adsorbed, then the solution was replaced by buffer solution with higher salt concentrations. For the brush substrate, the amounts of QPVP on the surface were 1.8 mg m^{-2} and Γ_0 was 4.2 mg m^{-2}. For the substrate with the preadsorbed QPVP, these numbers were 1.7 and 2.9 mg m^{-2}, respectively.

initially adsorbed HSA could be desorbed after 1.5 h exposure to buffer solution with as high a 0.15 M concentration of NaCl. These differences are summarized in Fig. 5. The dependence on NaCl ionic strength of the quantity of HSA adsorbed is shown. More HSA desorbed from both substrates, the higher the concentration of NaCl, but HSA was largely retained by the brush even in a buffer solution containing the extremely large ionic strength, 1 M NaCl.

Why was the rate of release of HSA from the two substrates so different? It is meaningful to suppose that rapid release of HSA from the preadsorbed QPVP layer indicated the absence of prominent steric impediment. In cases of competitive adsorption, the resulting pinning of adsorbed chains by other adsorbed chains has been much discussed and is known to generate sluggish desorption kinetics.[45,46] It

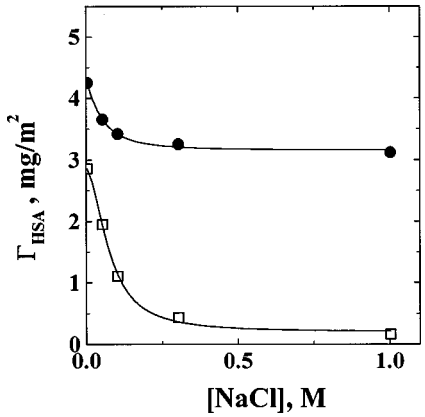

FIG. 5. Mass adsorbed of HSA is plotted against molar concentration of NaCl at a time 1 h after exposure to each NaCl solution. Other conditions are the same as in the caption of Fig. 4.

is interesting to conclude that these tendencies towards slowing down did not seem to hold for desorption from the QPVP preadsorbed layer: protein was quickly released from the adsorbed layer after individual segments were detached from the QPVP by the advent of small ions. The reason is probably rooted in the fact that negatively charged HSA globules tend to form layers on the top of oppositely charged preadsorbed QPVP rather than penetrate deeper towards the Si crystal surface (as in the case of polymer competition); this pattern of the adsorption evidently produced a lesser amount of kinetically restrictive pinned molecules.

However, slow release of this protein from the brush contrasts with the fast and almost complete release of polyglutamic acid from the same brush (this is described in detail elsewhere[47]). We hypothesize that sluggish release of HSA from the brush may stem from strong lateral hydrophobic interactions between the engulfed protein and the brush after a protein-brush complex forms.

Lateral interactions should be strengthened by QPVP chains between the protein globules. Support for this hypothesis comes from the vast literature on the polyelectrolyte-protein complexes. It is widely known that interaction of proteins with oppositely charged polyelectrolyte results in hydrophobization of the protein globule, and eventually phase separation above a given protein-polyelectrolyte molar ratio.[48,49] According to this scenario, hydrophobization of the HSA globules in the brush should dramatically increase lateral hydrophobic interactions in the adsorbed layer. This effect should be further enhanced by the large size of HSA molecule, since its smallest dimension is comparable to the average interchain spacing of the PVP grafted chains (25 Å for 1.8 mg m^{-2}). Entrapped in such a dense brush layer, HSA molecules had little diffusional freedom to escape from hydrophobic interactions and were simply stuck within the brush. But in a (thinner) statistically adsorbed layer, these tendencies should be less because the protein cannot become so fully engulfed.

One more point is evident in Fig. 5. As a function of increasing NaCl concentration in solution, decrease of the amount of HSA adsorbed was gradual, suggesting that HSA was adsorbed to both substrates with a distribution of binding energies. This distribution could stem from the inhomogeneity of the substrate, modified with QPVP molecules. Another possibility is lateral molecular inhomogeneity within the adsorbed layer; the HSA molecule is known to be partially hydrophobic. Heterogeneity of this kind may also originate from conformational distributions of the adsorbed protein molecules. Indeed, inhomogeneous adsorbed layers of chain molecules on apparently homogeneous substrates have been inferred for a wide range of neutral and charged polymers.[50–54] We cannot distinguish between these possibilities at this time.

Adsorption kinetics and adsorption isotherms

Figure 6 compares the time evolution of relative HSA adsorption (time-dependent amount adsorbed relative to the limiting amount adsorbed at longest times) for both substrates, with matched amounts of QPVP in both cases.

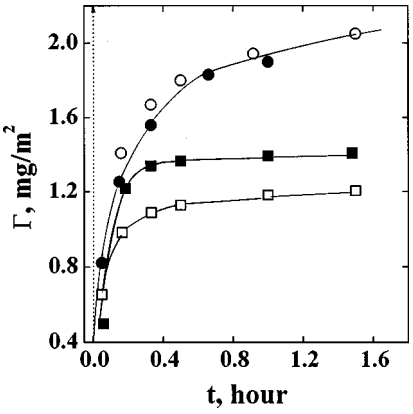

FIG. 6. Mass adsorbed of HSA is plotted against elapsed time for the adsorption of 0.02 mg mL^{-1} HSA in the brush (circles) and on the preadsorbed QPVP (squares). Amount of QPVP in the brush was 1.8 mg m^{-2} (filled circles) and 2.3 mg m^{-2} (open circles). For adsorption in the statistically adsorbed QPVP layer it was 1.2 mg m^{-2} (filled squares) and 1.7 mg m^{-2} (open squares). The buffer solution was the same as in Fig. 1, pD=9.2.

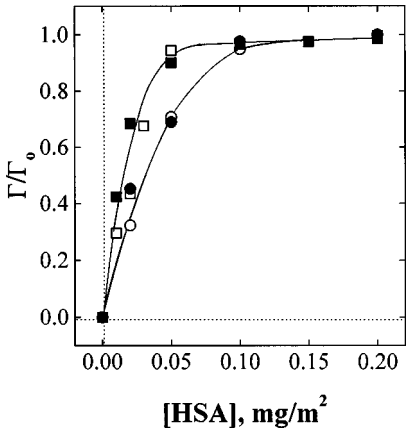

FIG. 7. Comparison of the adsorption isotherm of HSA for the brush substrates (circles) and the substrates with statistically preadsorbed QPVP (squares). In each comparison, the mass of HSA adsorbed was normalized by Γ_0, the saturated amount of protein in that experiment. Symbols and conditions are the same as in Fig. 6.

The striking feature in Fig.6 is that for the same concentration in solution, the quantity of HSA adsorbed approached the limiting value considerably more slowly for the brush substrates. At the same time, the total amount adsorbed was larger for the brush (when the amount of QPVP was matched for the substrates of two types); this was already discussed above (see Fig. 3). We suggest that kinetic differences between two substrates reflect the stronger steric hindrance to HSA diffusion imposed by the grafted QPVP chains.

To explain the difference in diffusional constraints between two substrates, it is meaningful to assume that the answer is rooted in the large dimensions of the HSA globule. As already mentioned, the HSA molecule can be considered either as a prolate ellipsoid of 14 nm×4 nm×4 nm dimensions[9,26] or as a triangular-shaped molecule with sides of 8 nm and average thickness of 3 nm.[24,44] A simple comparison of these dimensions with the mean shortest distance between QPVP chains (23.5 Å for the most dense brush with 2.0 mg m^{-2} adsorption) shows that geometrical restrictions must inevitably exist even if the HSA molecule entered the brush in its end-on configuration. The maximum amount of the protein adsorbed, 6.0 mg m^{-2}, is consistent with end-on orientation of HSA within the brush assuming prolate ellipoidal shape of the molecule,[9] or with more than two monolayers of end-on oriented molecules assuming triangular shape.[44] It is evident from our experiment that grafted QPVP chains formed relatively smaller and deeper ''pores'' and that the statistically-adsorbed QPVP chains formed more shallow and wider ''pores.'' The origin of the ''pores'' in the latter case was possibly tails of the molecules, which are known to extend from the surface to larger distances than loops.[55] We suggest though that side-on orientation (which is commonly found for the adsorption on the flat substrates[44]) might be realized on the statistically adsorbed QPVP surface, and some geometrical hindrance might also play some role in this latter case.

Formally, this retardation of influx is related to the classical restricted-diffusion theory developed for hard spheres.[56] A closer description may be Brownian motion of a polymer subject to rigid constraints as proposed by Fixman[57] and later developed by Zwanzig,[58] in which retardation of diffusion is rooted in changes of the shape of the diffusion channel (and, consequently, in changes of entropy of the adsorbate).

We are convinced, however, that uptake of the protein should also be strongly slowed by interaction of the HSA molecules with charged QPVP units. This effect is analogous to the known slow transport of linear polyelectrolytes in polymer networks of opposite charge.[59] In this scenario, no new molecules would be adsorbed from the solution until the portion of adsorbate molecules that were earlier bound to the outer plane of the brush had penetrated into deeper regions of the brush. Since the degree of polymerization of the grafted PVP chains was only 60, it is meaningful to assume that not more than one or two HSA molecules could be pushed into the spacing between grafted QPVP chains at any single lateral spot on the surface.

The restrictive factors discussed above might have not only kinetic, but also thermodynamic consequences for protein adsorption. Figure 7 summarizes the isotherms of HSA adsorption onto the substrates of both types. Note that the amount of QPVP on the surface was not varied in sufficiently wide limits to draw conclusions about the influence of the amount of QPVP as a source of charge on the substrate, but one notices striking differences between the substrates. For the same concentration of HSA in solution and matched amounts of QPVP on the surface, the relative uptake of the protein was considerably less within the brushes (which exhibited more rounded adsorption isotherms) than within the substrates containing statistically adsorbed QPVP. This is formally similar to the retardation of diffusion discussed above, but we suggest that it may have a different, thermodynamic, origin; an interesting possibility is that size-restriction considerations also limited the penetration depth of the HSA molecules into the substrates and that the latter was stronger for the brushes. This would make sense when one recalls that dimensions of the protein were equal to or exceeded the ''molecular pore'' dimension on the brush sur-

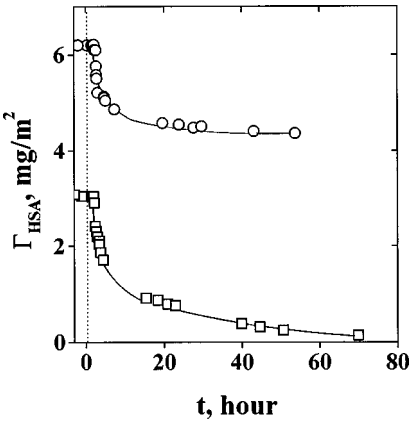

FIG. 8. Kinetics of the displacement of HSA by sodium polystyrene sulfonate, PSS. Desorption occurred from the brush substrate (open circles) and from the substrate with preadsorbed QPVP (open squares). The amount of QPVP grafted in the brush was 2.3 mg m^{-2}. The amount of QPVP statistically adsorbed was 1.7 mg m^{-2}. In both cases, HSA was first allowed to adsorb onto the substrate surfaces from 1 mg mL^{-1} solution at pD=9.2 (3 mM $Na_2B_4O_7^*10H_2O$) for 15 min so that the adsorbed layer was saturated with protein, then the protein solution was replaced momentarily by the pure buffer at this pD, and finally by 0.2 mg m^{-2} solution of PSS in the same buffer.

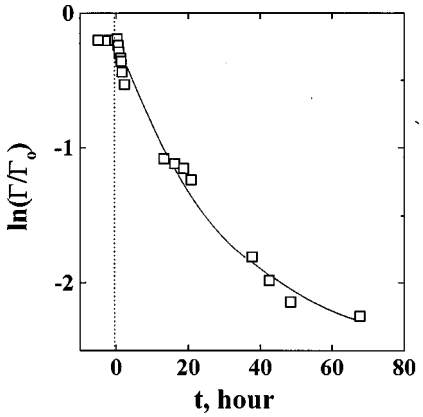

FIG. 9. Same experiment as in Fig. 8, but data for the substrate with preadsorbed QPVP are normalized by Γ_0, the amount of HSA adsorbed before the displacement by PSS, and plotted semilogarithmically as function of time. The data show curvature.

faces, and that faster kinetics (or larger ''molecular pores'') was found on the substrate with preadsorbed QPVP.

Displacement of adsorbed HSA by sodium polystyrene sulfonate

In order to further probe the adsorption of this protein, and its stability in response to change in the environment conditions, the ambient solution of HSA was replaced by a synthetic polymer of higher charge density and hence higher adsorption affinity. Control experiments showed that when both types of molecules competed for adsorption from a 50:50 mixture in the same solution, only the synthetic polymer adsorbed.

There were two advantages in using this polymer, PSS, as a displacer. First, the total binding energy of PSS is known to be the highest among known synthetic polyanions, presumably owing to the large nonelectrostatic contribution to its binding energy. A second advantage concerned the spectroscopic properties of PSS. PSS has a weak absorption band at 1599 cm^{-1}, which may be assigned to the conjugated $>SO_2$ stretching and in-plane stretching vibration of the benzene ring. This band does not overlap with the amide I region and its extinction coefficient is 160 times smaller that of the amide I band of HSA, so that these two bands could be reliably separated.

For PSS to adsorb, it was necessary for HSA to desorb. Figure 8 shows the time evolution of the amount of HSA adsorbed onto the substrates of both types, after the substrates bearing adsorbed HSA were brought into contact with buffered 0.2 mg mL^{-1}PSS solution. Again, one notices a striking difference between two substrates: the amount of protein desorbed from the preadsorbed QPVP layer was much larger. From the brush substrate, only ≈20% of HSA was displaced during the first 3 h of exchange, with almost no further change.

This small amount probably reflects protein molecules that were loosely bound with the upper layer of the brush; the major portion appears to have been irreversibly trapped within the brush. Possible reasons for this trapping were already discussed above (see discussion of Figs. 4 and 5). Note an additional factor which complicates the desorption of the HSA from the brush—it was harder for the large PSS ions than for small inorganic ions to reach PVP segments, which were located deeper in the brush because of blockade by the large protein molecules.

Though replacement of the HSA from the preadsorbed PVP layer took place more readily, desorption was nonetheless slow and complete displacement required an elapsed time of ≈70 h. Similarly slow kinetics was found earlier for the exchange of neutral and charged polymers at solid surfaces.[54,60,61] The common phenomenology suggests that slow reorganization in the layer of the adsorbed molecules was the limiting step in this kinetic process.

In prior work from this laboratory, quantitative analysis of the desorption kinetics showed that the desorption was exponential in the square root of elapsed time.[54,60,61] We applied similar analyses to the data in Fig. 8. An attempt to fit this data to an exponential relationship was unsuccessful; the data showed curvature (as shown in Fig. 9), indicating that kinetics was slower that exponential. However, data could be successfully fitted by the stretched exponential relationship, $\Gamma(t)/\Gamma_0 \sim \exp[-t/\tau_{off}]^{\beta}$ with $\beta=0.5$ (see Fig. 10). This is consistent with the previously proposed mechanism,[60,61] in which desorption is rate limited by diffusion away from the surface through other adsorbed chains, rather than rate limited by energetic detachment. Though the alternative mechanism, detachment-limit desorption, is still possible if one postulates heterogeneity within the adsorbed layer, it is unclear why heterogeneity should give $\beta=0.5$ rather than some other exponent.

OUTLOOK AND CONCLUSION

The main thrust of this study has been to compare protein adsorption at model surfaces with the same chemical makeup but different molecular architecture. We have de-

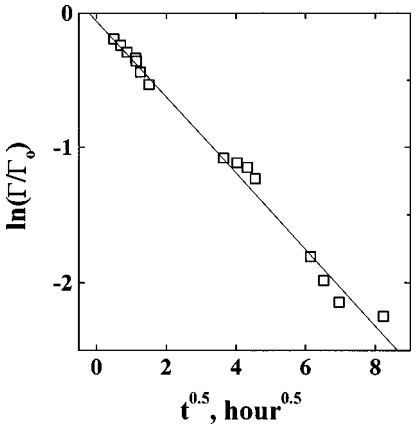

FIG. 10. Same data as in Fig. 8, but data for the substrate with preadsorbed QPVP are normalized by Γ_0, the amount of HSA adsorbed before the displacement by PSS, and plotted semilogarithmically as function of square root of time. One observes that data demonstrate a linear dependence, suggesting either adsorption heterogeneity or diffusion-limited desorption kinetics.

scribed differences in denaturation of the adsorbed HSA protein, differences in the adsorption rates, and differences in the tenacity of adsorption when the environmental conditions were changed to be less favorable. Perhaps the chief practical conclusion is that modification of the solid surface with a polyelectrolyte brush having the opposite charge of that of the protein produced irreversible (almost covalent-like) capture of these negatively charged biological molecules. These complexes were stable at physiological concentrations of salts ($\approx$0.15 M NaCl). This may find biotechnology application, for example in biosensor design.

[1] C. Schöneich, A. F. R. Hühmer, S. R. Rabel, J. F. Stobaugh, S. D. S. Jois, C. K. Larive, T. J. Siahaan, T. C. Squier, D. J. Bigelow, and T. D. Williams, Anal. Chem. **67**, 155 (1995).
[2] H. Yoshida, H. Nishihara, and T. Kataoka, Biotechnol. Bioeng. **43**, 1087 (1994).
[3] N. Kubota, M. Kounosu, K. Saito, K. Sugita, K. Watanabe, and T. Sugo, Biotechnol. Prog. **13**, 89 (1997).
[4] L. E. Weaver, Jr. and G. Carta, Biotechnol. Prog. **12**, 342 (1996).
[5] J. L. Ortega-Vinuesa and R. Hidalgo-Álvarez, Biotechnol. Bioeng. **47**, 633 (1995).
[6] K. Cammann, U. Lemke, A. Rohen, J. Sander, H. Wilken, and B. Winter, Angew. Chem. Int. Ed. Engl. **30**, 516 (1991).
[7] G. Decher, B. Lehr, K. Lowack, Y. Lvov, and J. Scmitt, Biosens. Bioelectron. **9**, 677 (1994).
[8] Y. Lvov, K. Ariga, I. Ichinose, and T. Kunitake, J. Am. Chem. Soc. **117**, 6117 (1995).
[9] M. E. Soderquist and A. G. Walton, J. Colloid Interface Sci. **75**, 386 (1980).
[10] W. Norde, F. MacRitchie, G. Nowicka, and J. Lyklema, J. Colloid Interface Sci. **112**, 447 (1986).
[11] R. K. Sandwick and K. J. Schray, J. Colloid Interface Sci. **115**, 130 (1987).
[12] Th. A. Horbett and J. L. Brash, in *Proteins at Interfaces: Physicochemical and Biomedical Studies*, edited by J. L. Brash and Th. A. Horbett ACS Symp. Ser. 343 (American Chemical Society, Washington, DC, 1987), p. 1.
[13] Th. J. Lenk, Th. A. Horbett, B. D. Ratner, and K. K. Chittur, Langmuir **7**, 1755 (1991).
[14] D. Kowalczyk, S. Slomkowski, and F. W. Wang, Polym. Prepr. (Am. Chem. Soc. Div. Polym. Chem.) **33**, 846 (1992).
[15] A. Kondo, F. Murakami, and K. Higashitani, Biotechnol. Bioeng. **40**, 889 (1992).
[16] T. Baniska, D. Kowalczyk, S. Slomkowski, and F. W. Wang, Polym. Prepr. (Am. Chem. Soc. Div. Polym. Chem.) **34**, 958 (1993).
[17] E. Lutanie, J. C. Voegel, P. Schaaf, M. Freund, J. P. Cazenave, and A. Schmitt, Proc. Natl. Acad. Sci. USA **89**, 9890 (1992).
[18] N. Kossovsky, A. Nguyen, K. Sukiassians, A. Festekjian, A. Gelman, and E. Sponsler, J. Colloid Interface Sci. **166**, 350 (1994).
[19] C.-S. Lee and G. Belfort, Proc. Natl. Acad. Sci. USA **86**, 8392 (1989).
[20] P. F. Brode III and D. S. Rauch, Langmuir **8**, 1325 (1992).
[21] P. B. Gaspers, C. R. Robertson, and A. Gast, Langmuir **10**, 2699 (1994).
[22] A. A. Karyakin, E. E. Karyakina, L. Gorton, O. A. Bobrova, L. A. Lukacheva, A. K. Gladilin, and A. V. Levashov, Anal. Chem. **68**, 4335 (1996).
[23] G. Walsh and D. Headon, *Protein Biotechnology* (Wiley, New York, 1994), p. 73.
[24] X. M. He and D. C. Carter, Nature (London) **358**, 209 (1992).
[25] D. Malamud and J. W. Drysdale, Anal. Biochem. **86**, 620 (1978).
[26] T. Peters, Adv. Protein Chem. **37**, 161 (1985).
[27] P. Frantz and S. Granick, Macromolecules **28**, 6915 (1995).
[28] S. Sukhishvili and S. Granick, Langmuir **13**, 4935 (1997).
[29] S. Sukhishvili and S. Granick, J. Chem. Phys. **109**, 6861 (1998).
[30] R. P. Sperline, S. Muralidharan, and H. Freiser, Langmuir **3**, 198 (1987).
[31] M.J. Azzorardi and H. Arribat, J. Adhes. **46**, 103 (1994).
[32] N. J. Harrick, J. Opt. Soc. Am. **55**, 851 (1965).
[33] H.G. Tompkins, Appl. Spectrosc. **28**, 335 (1974).
[34] P. T. T. Wong and K. Heremans, Biochim. Biophys. Acta **956**, 1 (1988).
[35] F. M. Wasacz, J. M. Olinger, and R. J. Jakobsen, Biochemistry **26**, 1464 (1987).
[36] R. B. Philp, D. J. L. McIver, and P. T. T. Wong, Biochim. Biophys. Acta **1021**, 9 (1990).
[37] L. Boulkanz, N. Balcar, and M.-H. Baron, Appl. Spectrosc. **49**, 1737 (1995).
[38] Yu. N. Chirgadze, E. V. Brazhnikov, and N. A. Nevskaya, J. Mol. Biol. **102**, 781 (1976).
[39] G. Zuber, S. J. Prestrelski, and K. Benedek, Anal. Biochem. **207**, 150 (1992).
[40] W. Norde, F. MacRitchie, G. Nowicka, and J. Lyklema, J. Colloid Interface Sci. **112**, 447 (1986).
[41] W. Norde, Adv. Colloid Interface Sci. **25**, 267 (1986).
[42] N. Kuramoto, M. Sakamoto, J. Komiyama, and T. Iijima, Makromol. Chem. **185**, 1419 (1984).
[43] G.K. Iwamoto, L. Winterton, R. S. Stoker, R. A. Van Wagenen, J. D. Andrade, and D. Mosher, J. Colloid Interface Sci. **106**, 459 (1985).
[44] E. Blomberg, P. M. Claesson, and R. D. Tilton, J. Colloid Interface Sci. **166**, 427 (1994).
[45] H. E. Johnson and S. Granick, Science **255**, 966 (1992).
[46] J. F. Douglas, H. E. Johnson, and S. Granick, Science **262**, 2010 (1993).
[47] S. Sukhishvili and S. Granick (unpublished).
[48] E. Tsuchida and K. Abe, in *Interactions between Macromolecules in Solution and Intermacromolecular Complexes* (Springer, New York, 1982), Chap. II.
[49] K. M. Clark and C. E. Glatz, Biotechnol. Prog. **3**, 241 (1987).
[50] H. M. Schneider, S. Granick, and S. Smith, Macromolecules **27**, 4721 (1994).
[51] P. Frantz and S. Granick, Macromolecules **27**, 2553 (1994).
[52] H. Tanaka, A. Swerin, and L. Ödberg, Langmuir **10**, 3466 (1994).
[53] N. G. Hoogeveen, M. A. Cohen Stuart, and G. J. Fleer, J. Colloid Interface Sci. **182**, 146 (1996).
[54] S. Sukhishvili and S. Granick, J. Chem. Phys. **109**, 6869 (1998).
[55] G. J. Fleer, M. A. Cohen Stuart, J. M. H. M. Scheutjens, T. Cosgrove, and B. Vincent, *Polymers at Interfaces* (Chapman & Hall, London, 1993).
[56] C. P. Bean, in *Membranes*, edited by G. Eisenman (Dekker, New York, 1972), pp. 1–54.
[57] M. Fixman, J. Chem. Phys. **69**, 1527 (1978).
[58] R. Zwanzig, J. Phys. Chem. **96**, 3926 (1992).
[59] A. M. Chupyatov, V. B. Rogacheva, A. B. Zezin, and V. A. Kabanov, Polym. Prepr. (Am. Chem. Soc. Div. Polym. Chem.) **36**, 169 (1994).
[60] H. E. Johnson and S. Granick, Science **255**, 966 (1992).
[61] J. F. Douglas, H. E. Johnson, and S. Granick, Science **262**, 2010 (1993).